Journal of Physics: Complexity

LETTER

Explosive transitions in epidemic dynamics

Georg Börner[1,6], Malte Schröder[1,6], Davide Scarselli[2], Nazmi Burak Budanur[2,3], Björn Hof[2] and Marc Timme[1,4,5,*]

[1] Chair for Network Dynamics, Center for Advancing Electronics Dresden (cfaed) and Institute of Theoretical Physics, Technische Universität Dresden, Dresden 01062, Germany
[2] Institute of Science and Technology Austria, Klosterneuburg, Austria
[3] Max Planck Institute for the Physics of Complex Systems, Dresden, Germany
[4] Cluster of Excellence Physics of Life, Technische Universität Dresden, Dresden 01062 Germany
[5] Lakeside Labs, Lakeside B04b, 9020 Klagenfurt, Austria
[6] These authors contributed equally.
[*] Authors to whom any correspondence should be addressed.

E-mail: marc.timme@tu-dresden.de

Keywords: phase transitions, epidemic dynamics, SIR model, explosive transitions, third-order transition

Supplementary material for this article is available online

OPEN ACCESS

RECEIVED
15 September 2022

REVISED
30 September 2022

ACCEPTED FOR PUBLICATION
12 October 2022

PUBLISHED
25 October 2022

Abstract

Standard epidemic models exhibit one continuous, second order phase transition to macroscopic outbreaks. However, interventions to control outbreaks may fundamentally alter epidemic dynamics. Here we reveal how such interventions modify the type of phase transition. In particular, we uncover three distinct types of explosive phase transitions for epidemic dynamics with capacity-limited interventions. Depending on the capacity limit, interventions may (i) leave the standard second order phase transition unchanged but exponentially suppress the probability of large outbreaks, (ii) induce a first-order discontinuous transition to macroscopic outbreaks, or (iii) cause a secondary explosive yet continuous third-order transition. These insights highlight inherent limitations in predicting and containing epidemic outbreaks. More generally our study offers a cornerstone example of a third-order explosive phase transition in complex systems.

1. Introduction

Phase transitions separate qualitatively different collective states emerging in large complex systems [1–6]. Many models of complex systems dynamics, for instance the standard susceptible-infected-recovered (SIR) model of epidemic dynamics and models of random percolation, exhibit a single phase transition that often is second order and thus continuous [7–9]. For epidemic spreading dynamics, a continuous transition implies that the total number of individuals infected during an epidemic continuously varies with the infectiousness.

Previous research has shown that complex systems may exhibit more intricate and involved collective dynamics and include discontinuous or explosive transitions if the settings become strongly nonlinear, severely constrained or heterogeneous. Examples include a strong dependence of the epidemic transition on the connectivity in structured populations with scale-free interaction topology [10, 11], epidemics where treatment options are limited by resource availability [12] and discontinuous hybrid phase transitions of co-evolving epidemics of two or more diseases [13, 14]. Recent related results for explosive percolation processes, however, indicate that such explosive transitions might only appear discontinuous in finite size systems but are often continuous with non-standard critical exponents [15–22].

In this Letter, we demonstrate that capacity-limited interventions may induce explosive transitions that may appear discontinuous but in fact are third-order.

The COVID-19 pandemic has highlighted the importance of interventions such as testing, contact tracing and vaccinations to control the spread of epidemics [23]. Importantly, the limited capacity of such interventions restricts their capability to contain epidemic outbreaks, especially when the time scales of test or vaccination rates are similar to those of the disease spread and progression. Recent empirical observations and modeling studies [12, 23–25] suggest that interventions may prevent outbreaks or reduce their size, yet

total case numbers may rapidly increase once the intervention capacity limit is reached, leading to sudden explosive and apparently discontinuous transitions to large outbreaks. However, the exact type of phase transitions and the mechanisms underlying them remain unclear.

Here, we uncover explosive phase transitions emerging in epidemic models with limited-capacity interventions. We find three distinct types of transitions depending on the scaling of the intervention capacity with the total population size. We clarify the mechanisms underlying these transitions by providing generic arguments under which conditions these transitions emerge, valid for a broad class of models. More generally, our results highlight an example of a third-order explosive phase transition in a generic complex system.

2. Results

In the standard SIR model, susceptible (S) individuals become infected (I) with rate $\beta SI/N$ and are removed or recover (R) with a rate γI (figures 1(a)–(e)). Here, we denote both the states and the absolute number of individuals in that state with capital letters S, I and R. $\beta I/N$ denotes the infection rate per individual and γ denotes the recovery rate per individual. The basic reproduction number $R_0 = \beta/\gamma$ quantifies the expected secondary infections caused by a single infected in a fully susceptible population and characterizes the qualitative collective dynamics of the model. If $R_0 < R_c^{(1)} = 1$, the number of infected individuals $I(t)$ on average exponentially decreases with time t. If $R_0 > R_c^{(1)}$, it initially increases exponentially. As a result, in the limit of an infinitely large population $N \to \infty$, a macroscopic outbreak occurs and ultimately affects some positive fraction $i_{\text{tot}} = \lim_{N\to\infty} I_{\text{tot}}/N > 0$ of the total population, where $I_{\text{tot}} = \lim_{t\to\infty}[R(t) + Q(t)] = I_{\text{tot}} = N - \lim_{t\to\infty} S(t)$ describes the total number of individuals ever infected. This relative total outbreak size i_{tot} serves as an order parameter, distinguishing the two regimes, and is implicitly given by [9]

$$i_{\text{tot}} = 1 - e^{-R_0\, i_{\text{tot}}} \tag{1}$$

with a solution $i_{\text{tot}} > 0$ only above a critical reproduction rate, $R_0 > R_c^{(1)} = 1$, compare figure 1(e).

We modify the standard SIR model to include capacity-limited interventions by adding a single new state (Q) (e.g. quarantine or treatment), see figures 1(f)–(j) for an illustration of this SIRQ model. In addition to the standard state transitions, infected individuals are removed into a state Q at an additional rate δI but at most at a rate κ, denoting the intervention capacity in units of individuals per time. The microscopic dynamics of both models follows a stochastic process where all transitions occur as independent Poisson processes at their given rates. These dynamics determine the probability $\mathcal{P}$ of an outbreak when a single individual is initially infected (compare figures 1(d) and (i)). The macroscopic dynamics in the limit of infinitely large populations, $N \to \infty$ are described by the mean field rate equations

$$\begin{aligned} \frac{\mathrm{d}s}{\mathrm{d}t} &= -\beta s i \\ \frac{\mathrm{d}i}{\mathrm{d}t} &= \beta s i - \gamma i - \min\left[\delta i, \lim_{N\to\infty} \kappa/N\right], \end{aligned} \tag{2}$$

where the lower case letters s, i and r denote the fraction of individuals in the corresponding state, e.g. $s = \lim_{N\to\infty} S/N$. These dynamics govern the relative total outbreak size i_{tot} if a macroscopic outbreak occurs. We numerically illustrate our arguments and calculations for parameters $\gamma = \delta = 1$ for clarity of presentation and change the infection rate β to vary R_0.

Compared to the standard SIR model, the interventions shift the critical point because infected individuals are additionally removed into state Q. Macroscopic outbreaks only occur when $R_0 > R_c^{(2)} > 1$ (compare figures 1(e) and (j)). Once the reproduction number even slightly crosses a second threshold $R_c^{(3)} > R_c^{(2)}$, the total number of infected surges dramatically (figure 1(j)). In contrast to the smooth changes with the reproduction number in the standard SIR model (figures 1(b) and (c)), such explosive transitions may pose major challenges for predictability and control of epidemic dynamics. Small changes such as stochastic number fluctuations in finite size systems or small deviations in the reproduction number may yield large qualitative changes in the epidemic dynamics (figure 1(h)).

Do these capacity-limited interventions create a discontinuous transition in the epidemic dynamics? As long as $I(t) < I_c = \kappa/\delta$, infected individuals recover at an effective rate $\gamma_{\text{eff}} I = (\gamma + \delta) I = 2I$. The expected dynamics of the system are described by an effective reproduction number $R_{\text{eff}} = \beta/\gamma_{\text{eff}} = R_0/2$. Consequently, we expect the critical point above which macroscopic outbreaks occur to be shifted to $R_c^{(2)} = 1 + \delta/\gamma = 2$. If at any time there are more infected individuals, $I(t) > I_c$, the effective recovery rate reduces to $\gamma_{\text{eff}} I = \gamma I + \kappa < 2I$. To understand how this change affects the epidemic dynamics, we consider

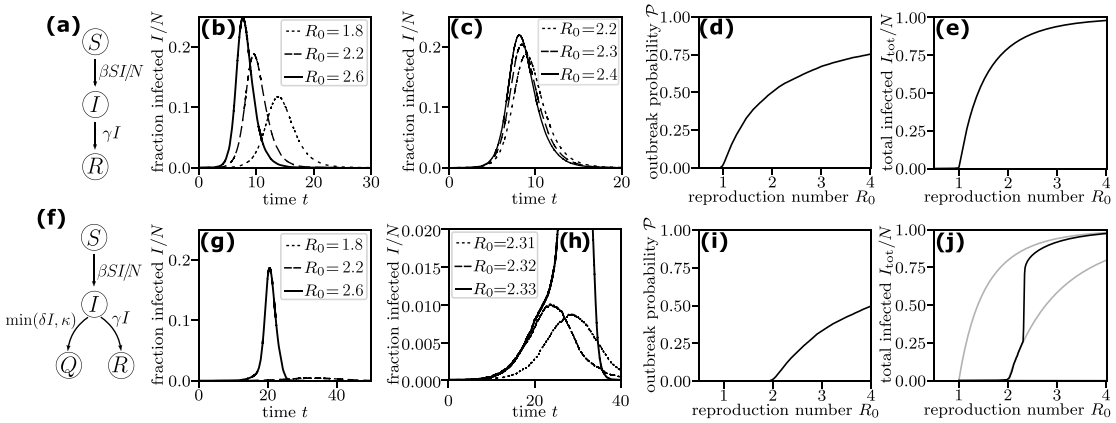

Figure 1. Impact of capacity-limited interventions on epidemic spreading processes. Dynamics of the standard SIR model (a)–(e) and a model with capacity-limited interventions (SIRQ model, panels (f)–(j)). (a), (f) Compartment model sketch of both models. (b), (c), (g), (h) Dynamics of the number of currently infected $I(t)$ during a typical outbreak for three reproduction numbers R_0, each starting from $I_1(0) = 10$ initially infected. Outbreak dynamics change smoothly in the SIR model (b), (c) but vary much more strongly under the influence of interventions (g), (h). (d), (i) The outbreak probability $\mathcal{P}$ quantified by the fraction of realizations with a large number $I_{\text{tot}} > \sqrt{N}$ of total infected out of 10^4 realizations, each with $I_1(0) = 1$. Without interventions, large outbreaks emerge already for $R_0 > R_c^{(1)} = 1$ (panel (d)); interventions strongly suppress the outbreak probability as long as $R_0 < R_c^{(2)} = 2$ (panel (i)). (e), (j) The average total size of outbreaks grows continuously from zero once $R_0 > R_c^{(1)}$ for the SIR model without interventions or $R_0 > R_c^{(2)}$ for the SIRQ model, respectively. With limited intervention capacity, a secondary transition emerges at $R_c^{(3)} > R_c^{(2)}$, where the number of total infected grows dramatically upon a small increase in the basic reproduction number R_0, quickly approaching the outbreak size expected without interventions. This transition is reflected in the strong variation of the time evolution (panel (h)) near $R_c^{(3)}$. Grey lines indicate the expected number of infected in the standard SIR model and with unlimited intervention capacity $\kappa \to \infty$, respectively. All results are illustrated for total population size $N = 10^6$, recovery rate $\gamma = 1$, $\delta = 1$, and intervention capacity $\kappa = 10^4$.

the early microscopic spreading dynamics. With a single initially infected individual, the number of currently infected changes by $+1$ or -1 with each infection or recovery event, respectively. The probability for each event is proportional to the rates of the respective state transitions. Even if the number of infected should decrease on average and we would expect the epidemic to die out, there is a non-zero probability to reach any number of currently infected $I(t) \leqslant N$.

The early dynamics if $I(t)$ ever becomes larger than I_c is thus equivalent to the Gambler's Ruin threshold crossing problem, see supplemental material for a more detailed description. In the following, we reveal three distinct phase transitions depending on the scaling of the intervention capacity with the population size, $\kappa \propto N^\alpha$.

2.1. Constant intervention capacity

For constant $\kappa \propto N^0$, the system exhibits some positive probability of reaching $I > I_c$. While this probability is exponentially suppressed with increasing intervention capacity κ, the interventions cannot completely prevent outbreaks. Once the number of infected becomes sufficiently large, the constant intervention rate κ becomes negligible compared to the natural recovery rate γI and the system behaves like a standard SIR model without interventions. Consequently, macroscopic outbreaks occur with positive probability as soon as $R_0 > R_c^{(1)} = 1$, similar to the standard SIR model, but the outbreak probability is exponentially suppressed with the intervention capacity κ (figure 2(a)). The macroscopic dynamics of the outbreaks that do occur is determined by the rate equation (2). The size of an outbreak (when it does occur) is thus the same as in the standard SIR model (compare figures 3(a) and (b)).

2.2. Sublinear intervention capacity

For sublinearly scaling intervention capacity $\kappa \propto N^\alpha$ with $0 < \alpha < 1$, the same argument for the microscopic dynamics applies. However, now the threshold value $I_c = \kappa/\delta \propto N^\alpha$ grows with the population size. Thus, the probability for the outbreak to grow beyond this threshold becomes zero in the large population limit $N \to \infty$ as long as the effective reproduction number $R_{\text{eff}} = R_0/2 < 1$, i.e. as long as $R_0 < R_c^{(2)} = 1 + \delta/\gamma = 2$. Only then can macroscopic outbreaks occur with a finite probability (figure 2(b)). When a macroscopic outbreak does occur, the intervention rate becomes negligible since it scales sublinearly with the population size, $\kappa/N \to 0$ as $N \to \infty$. The dynamics is equivalent to the standard SIR model. Consequently, we observe a discontinuous transition of the outbreak size at $R_c^{(2)} = 1 + \delta/\gamma = 2$ (figures 3(c) and (d)).

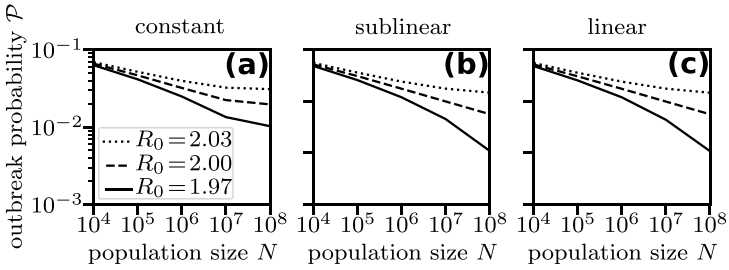

Figure 2. Growing intervention capacity delays macroscopic outbreaks. The outbreak probability $\mathcal{P}$, computed as the fraction of realizations that reach $I_{\rm tot} > \sqrt{N}$ out of 10^5 total realizations from one initially infected, $I_1(0) = 1$, behaves qualitatively differently for constant and (sub)linearly scaling intervention capacity. (a) For constant intervention capacity ($\kappa = 100$), the outbreak probability settles to non-zero values for any $R_0 > R_{\rm c}^{(1)} = 1$. (b), (c) For sublinear and linear intervention capacity ($\kappa = \sqrt{N}$ and $\kappa = 0.01\,N$, respectively), the outbreak probability goes to zero for $R_0 < R_{\rm c}^{(2)} = 2$ in the limit of infinitely large populations; interventions prevent outbreaks. At the critical point $R_{\rm c}^{(2)} = 2$ the outbreak probability decreases as a power law as $N \to \infty$. Note that due to defining outbreaks by $I_{\rm tot} > \sqrt{N}$, and our choice of $\kappa = \sqrt{N}$ and $\kappa = 0.01\,N \geqslant \sqrt{N}$ for $N \geqslant 10^4$, the outbreak probability for sublinear and linear scaling is identical since in both cases the intervention capacity is equal to or larger than our outbreak threshold. All results are shown for recovery rate $\gamma = 1$ and $\delta = 1$.

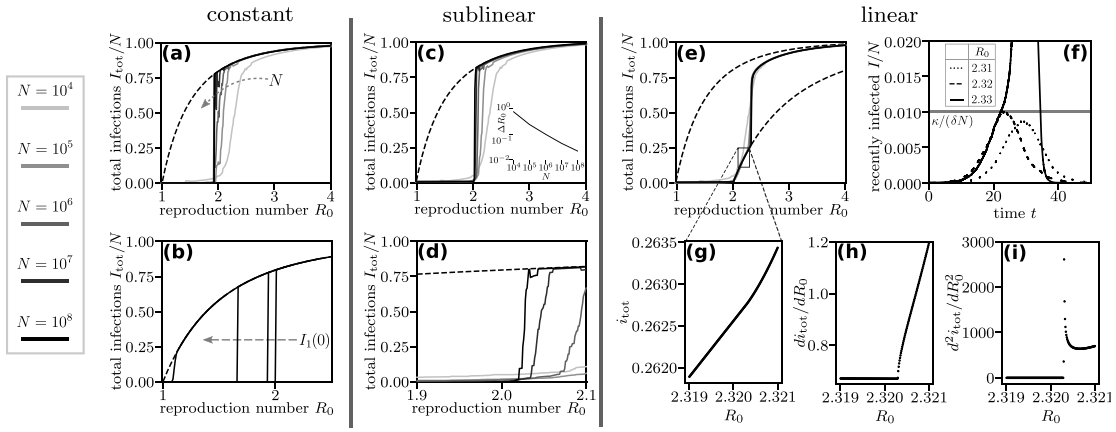

Figure 3. Limited quarantine induces different explosive transitions. (a), (b) For constant intervention capacity $\kappa = 100$, only few outbreaks are observed for $R_0 < R_{\rm c}^{(2)} = 1 + \delta/\gamma = 2$ due to the small outbreak probability (panel (a), compare figure 2(a)). Outbreaks that do occur quickly grow to the same size as for standard SIR dynamics without interventions (dashed line), as also demonstrated by increasing the number of initially infected ($I_1(0) \in \{1, 10, 100, 1000\}$ for $N = 10^8$, panel (b)). (c), (d) For sublinear intervention capacity, $\kappa = N^{1/2}$, no outbreaks occur for $R_0 < R_{\rm c}^{(2)} = 1 + \delta/\gamma = 2$ in the thermodynamic limit (compare figure 2(b)). For $R_0 > R_{\rm c}^{(2)}$, the outbreak size is close to that of SIR dynamics without intervention (dashed line). At the critical point $R_0 = R_{\rm c}^{(2)}$, the outbreak size increases discontinuously in the thermodynamic limit $N \to \infty$. (c, inset) The width $\Delta R_0 = R_0^+ - R_0^-$ of the transition region in which the total number of infected increases from $I_{\rm tot}(R_0^-)/N = 0.1$ to $I_{\rm tot}(R_0^+)/N = 0.75$ decays to zero as $N \to \infty$. (e), (f) For linear intervention capacity $\kappa = 0.01\,N$, no outbreaks occur for $R_0 < R_{\rm c}^{(2)} = 1 + \delta/\gamma = 2$ in the thermodynamic limit (compare figure 2(c)). Above $R_{\rm c}^{(2)} = 1 + \delta/\gamma = 2$ the outbreak size is initially the same as in the standard SIR model with increased effective recovery rate $\gamma + \delta$ (compare figure 1(j)). At a second critical point $R_{\rm c}^{(3)} \approx 2.3203$, where the concurrent number of infected during the outbreak overwhelms the intervention capacity ($I(t) > \kappa/\delta$, panel (f)), the outbreak size undergoes a second, sudden but continuous transition. (g)–(i) The fraction of total infected $i_{\rm tot}$ computed from the mean-field rate equation (2) and its derivatives reveal a continuous third-order transition at $R_{\rm c}^{(3)}$ where only the second derivative $d^2 i_{\rm tot}/dR_0^2$ is discontinuous. All outbreak sizes are evaluated as averages over large outbreaks with $I_{\rm tot} > \sqrt{N}$ over at least 100 realizations with $I_1(0) = 10$ initially infected (unless explicitly stated otherwise). All results are shown for recovery rate $\gamma = 1$ and $\delta = 1$.

2.3. Linear intervention capacity

For linear intervention capacity $\kappa = \tilde{\kappa} N \propto N$ with constant $\tilde{\kappa}$, the dynamics become more intriguing. Again, the same argument for the microscopic dynamics applies as for the sublinearly scaling intervention capacity. Macroscopic outbreaks are only possible for $R_0 > R_{\rm c}^{(2)} = 1 + \delta/\gamma = 2$ (figure 2(c)). However, sufficiently small macroscopic outbreaks do not immediately exceed the intervention capacity threshold $I_{\rm c} \propto N$, and I remains smaller than $I_{\rm c}$ during the outbreak. We thus observe a continuous second order transition equivalent to an SIR model with recovery rate $\gamma_{\rm eff} = (\gamma + \delta) = 2$. Only if the reproduction number is larger than a second critical value, $R_0 > R_{\rm c}^{(3)}$, the concurrently infected exceed the threshold $I_{\rm c}$ during the outbreak and a second transition occurs.

To reveal the type of the second transition, we compute the scaling of the number of additionally infected when the intervention capacity is overwhelmed. We here sketch the main steps in the argument, a step-by-step calculation is provided in the supplemental material. We focus on the time t^* at which the number of infected first exceeds the threshold $I(t^*) = I_c$, or equivalently $i(t^*) = I_c/N = \tilde{\kappa}/\delta$. Until t^*, the dynamics are identical to a system with infinite intervention capacity $\kappa \to \infty$ with $i_\infty(t)$ infected. Exactly at t^* both $i(t^*)$ and its first derivative are still the same as for infinite intervention capacity (equation (2)), but the second derivative changes to the right of t^*. Compared to a system with infinite intervention capacity, as $t \to t^*$ we find

$$\begin{aligned} i(t) - i_\infty(t) &\sim \frac{1}{2}\left[i''(t^*) - i''_\infty(t^*)\right](t-t^*)^2 \\ &\propto \left(R_0 - R_c^{(3)}\right)^{1/2}(t-t^*)^2. \end{aligned} \tag{3}$$

However, the number of infected remains above the threshold only for a short time $\Delta t \propto (R_0 - R_c^{(3)})^{1/2}$, following from the quadratic expansion around the maximum of $i(t)$ which increases linearly with $(R_0 - R_c^{(3)})$ (see supplemental material for details). We then find the leading order scaling of the additional infections by integrating the additional infection rate $\beta s(t)\left[i(t) - i_\infty(t)\right]$ for the time Δt, resulting in a leading order correction proportional to $\left[i''(t^*) - i''_\infty(t^*)\right]\Delta t^3 \propto (R_0 - R_c^{(3)})^2$. Secondary infections enter only as higher order corrections. The explosive nature of the transition emerges from a very large prefactor of the additional term, scaling as κ^{-6} and thus resulting in a very sudden increase in the total number of infected individuals especially for small intervention capacities. We thus find that the second derivative of $i_{\text{tot}}(R_0)$ is discontinuous at $R_0 = R_c^{(3)}$ and the transition is sudden, yet third-order, and thus surprisingly even smoother than the second order transition at $R_c^{(2)}$ (figures 3(e)–(i)).

3. Discussion

The above explanations remain qualitatively valid for a broad class of systems since they only rely on scaling arguments to understand the impact of the limited intervention capacity on the microscopic dynamics and generic leading order behavior for the effect on the macroscopic dynamics. Our argument only requires that: (i) The system exhibits non-trivial outbreak dynamics even with infinite intervention capacity, ensuring that outbreaks exist in the first place if the intervention capacity scales with the population size. (ii) The intervention capacity enters the macroscopic dynamics as a hard limit such that the derivative of $i(t)$ is continuous but not differentiable when the number of infected overwhelms the intervention capacity (compare equation (2)). In other cases, the dynamics may arbitrarily closely approximate the phase transition observed here but the fraction of infected changes smoothly with the reproduction number R_0.

In the supplemental material, we present a range of simple and more complex model variations illustrating these conditions and the robustness of the reported transitions. In particular, we (a) highlight the necessity of both conditions to observe the third-order transition by analyzing small variations of the model that do not fulfill one of the two conditions, and (b) demonstrate the universality of our arguments by analyzing various similar models including, for example, additional infected states, partially effective interventions, or explicit time delays between testing and intervention, that all show the same qualitative dynamics.

Overall, our results offer a novel perspective on epidemic containment with capacity-limited countermeasures. The different types of explosive transitions to large outbreaks present different challenges for the predictability and control of epidemic dynamics. This applies in particular to the evaluation of containment measures across cities or countries when the intervention capacity depends on the population size.

They also highlight the option of novel types of simultaneously explosive as well as third-order phase transitions in complex systems in general.

Data availability statement

The data that support the findings of this study are available from the corresponding author upon reasonable request.

Acknowledgments

We acknowledge support from the Volkswagen Foundation under Grant No. 99720 and the German Federal Ministry for Education and Research (BMBF) under Grant No. 16ICR01. This research was supported by the

Deutsche Forschungsgemeinschaft (DFG, German Research Foundation) under Germany's Excellence Strategy—EXC-2068—390729961—Cluster of Excellence Physics of Life of TU Dresden.

ORCID iDs

Georg Börner https://orcid.org/0000-0003-3784-9764
Malte Schröder https://orcid.org/0000-0001-8756-9918
Davide Scarselli https://orcid.org/0000-0001-5227-4271
Nazmi Burak Budanur https://orcid.org/0000-0003-0423-5010
Björn Hof https://orcid.org/0000-0003-2057-2754
Marc Timme https://orcid.org/0000-0002-5956-3137

References

[1] Anderson R M and May R M 1992 *Infectious Diseases of Humans: Dynamics and Control* (Oxford: Oxford University Press)
[2] Daley D J and Gani J 2001 *Epidemic Modelling: An Introduction* vol 15 (Cambridge: Cambridge University Press)
[3] Huang K 2009 *Introduction to Statistical Physics* (Boca Raton, FL: CRC Press)
[4] Wolf F and Geisel T 1998 Spontaneous pinwheel annihilation during visual development *Nature* **395** 73
[5] Timme M and Schröder M 2020 Disentangling scaling arguments to empower complex systems analysis *Nat. Phys.* **16** 1086
[6] Sethna J 2021 *Statistical Mechanics: Entropy, Order Parameters and Complexity* vol 14 (Oxford: Oxford University Press)
[7] Kermack W O and McKendrick A G 1927 A contribution to the mathematical theory of epidemics *Proc. R. Soc.* A **115** 700
[8] Hethcote H W 2000 The mathematics of infectious diseases *SIAM Rev.* **42** 599
[9] House T 2012 Modelling epidemics on networks *Contemp. Phys.* **53** 213
[10] Eguíluz V M and Klemm K 2002 Epidemic threshold in structured scale-free networks *Phys. Rev. Lett.* **89** 108701
[11] Nielsen B F, Simonsen L and Sneppen K 2021 COVID-19 superspreading suggests mitigation by social network modulation *Phys. Rev. Lett.* **126** 118301
[12] Böttcher L, Woolley-Meza O, Araújo N A, Herrmann H J and Helbing D 2015 Disease-induced resource constraints can trigger explosive epidemics *Sci. Rep.* **5** 16571
[13] Cai W, Chen L, Ghanbarnejad F and Grassberger P 2015 Avalanche outbreaks emerging in cooperative contagions *Nat. Phys.* **11** 936
[14] Grassberger P, Chen L, Ghanbarnejad F and Cai W 2016 Phase transitions in cooperative coinfections: simulation results for networks and lattices *Phys. Rev.* E **93** 042316
[15] Achlioptas D, D'Souza R M and Spencer J 2009 Explosive percolation in random networks *Science* **323** 1453
[16] Nagler J, Levina A and Timme M 2011 Impact of single links in competitive percolation *Nat. Phys.* **7** 265
[17] da Costa R A, Dorogovtsev S N, Goltsev A V and Mendes J F F 2010 Explosive percolation transition is actually continuous *Phys. Rev. Lett.* **105** 255701
[18] Riordan O and Warnke L 2011 Explosive percolation is continuous *Science* **333** 322
[19] Grassberger P, Christensen C, Bizhani G, Son S-W and Paczuski M 2011 Explosive percolation is continuous, but with unusual finite size behavior *Phys. Rev. Lett.* **106** 225701
[20] Schröder M, Rahbari S E and Nagler J 2013 Crackling noise in fractional percolation *Nat. Commun.* **4** 2222
[21] D'Souza R M and Nagler J 2015 Anomalous critical and supercritical phenomena in explosive percolation *Nat. Phys.* **11** 531
[22] D'Souza R M, Gómez-Gardeñes J, Nagler J and Arenas A 2019 Explosive phenomena in complex networks *Adv. Phys.* **68** 123
[23] Scarselli D, Budanur N B, Timme M and Hof B 2021 Discontinuous epidemic transition due to limited testing *Nat. Commun.* **12** 2586
[24] Vyska M and Gilligan C 2016 Complex dynamical behaviour in an epidemic model with control *Bull. Math. Biol.* **78** 2212
[25] Di Muro M A, Alvarez-Zuzek L G, Havlin S and Braunstein L A 2018 Multiple outbreaks in epidemic spreading with local vaccination and limited vaccines *New J. Phys.* **20** 083025